Effect of Interfacial Molecular Orientation on Power Conversion Efficiency of Perovskite Solar Cells

Minyu Xiao[1], Suneel Joglekar[2], Xiaoxian Zhang[3], Joshua Jasensky[1], Jialiu Ma[1], Qingyu Cui[2], L. Jay Guo[2], Zhan Chen[1]**

[1]*Department of Chemistry, University of Michigan, Ann Arbor, Michigan, 48109, USA*

[2]*Department of Electrical Engineering and Computer Science, University of Michigan, Ann Arbor, Michigan, 48109, USA*

[3] *CAS Key laboratory of Standardization and Measurement for Nanotechnology, Chinese Academy of Sciences Center for Excellence in Nanoscience, National Center for Nanoscience and Technology, Beijing 100190, China*

[*]*Corresponding author: L. Jay Guo (guo@umich.edu), Zhan Chen (zhanc@umich.edu)*

1. SFG experiment:

The SFG spectrometer used in this research is a commercial product from EKSPLA. It is composed of a pico-second Nd:YAG laser, a nonlinear optical system, and a detection system. The laser beams used for SFG experiments are a 20 ps 20 Hz visible beam at 532 nm and a frequency tunable infrared (IR) beam. In an SFG experiment, SFG spectra were collected by overlapping the visible (532nm) beam and the tunable IR beam on the sample surface, at incident angles of 60° and 55° respectively (versus the surface normal). The visible and IR beams are both spatially and temporally aligned in order to generate the sum frequency signal from the interface. In this study, SFG spectra with different polarization combinations of the input and signal beams (ssp and sps) were collected, where ssp represents s-polarized sum frequency output, s-polarized visible input and p-polarized infrared input; sps represents s-polarized sum frequency output, p-polarized visible input and s-polarized infrared input. SFG spectra were collected from layered thin films as shown in Figure 2c in the main text.

2. Bandgap alignment of perovskite solar cell fabricated:

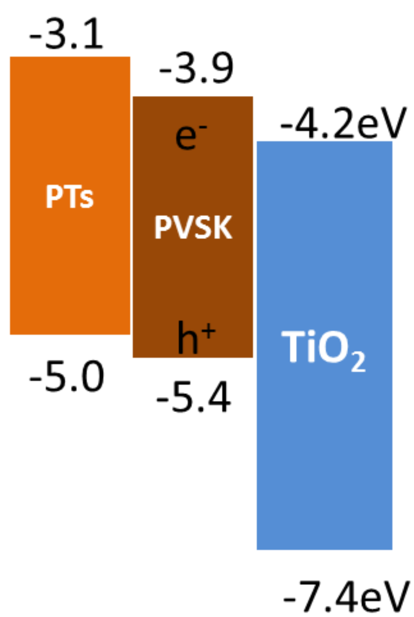

Figure S1. Schematic of bandgap alignment.

3. SCLC of different PT layer:

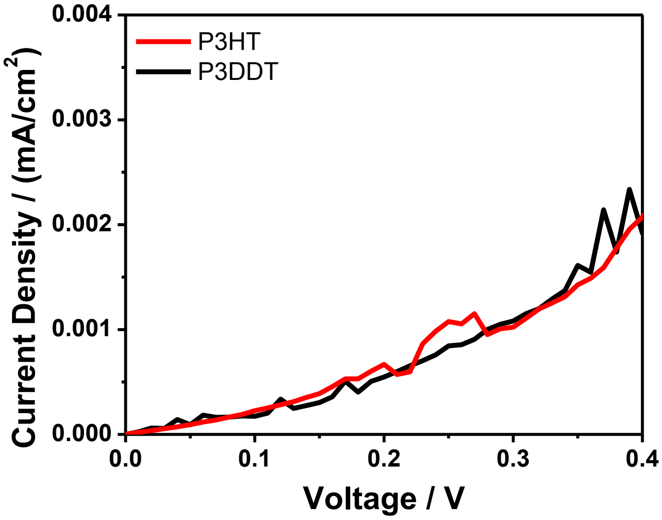

Figure S2 SCLC of PT derivatives in an ITO/PT/Au sandwiched structure

4. GIXRD of P3HT on perovskite surface:

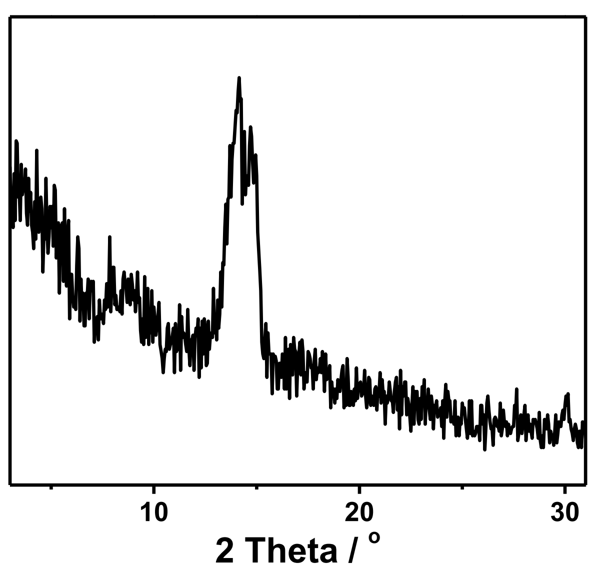

Figure S3 GIXRD spectrum of P3HT on perovskite surface

GIXRD is a thin film sensitive x-ray diffraction technique (in comparison to powder XRD). Here no obvious P3HT 100 peak around 5.2° was detected in the GIXRD spectrum. The main peaks observed in GIXRD originate from the perovskite 110 plane (around 15°), and the 220 crystal plane (30°). The GIXRD result shown here supports the XRD results reported in the main text, indicating that the PT layer is quite amorphous.

5. Perovskite thin film structure

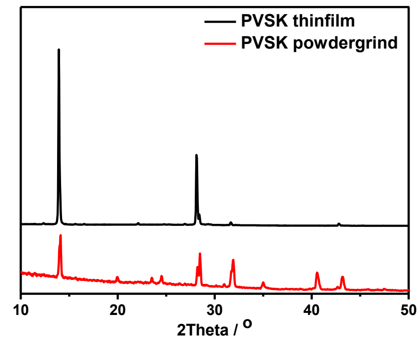

Figure S4 XRD spectra of pristine perovskite thin film and powder-ground perovskite thin film

6. Detailed fitting parameter of SFG spectrum in Figure 3:

	1435 cm^{-1} Peak	
	Peak width	Peak Amplitude
P3HT ssp 100nm	22.0	7.48
P3HT ssp 60nm	22.2	5.50
P3HT sps 100nm	22.1	6.85
P3HT sps 60nm	21.9	5.91

	1435 cm^{-1} Peak	
	Peak width	Peak Amplitude
P3OT ssp 100nm	22.0	9.68
P3OT ssp 60nm	22.0	7.26
P3OT sps 100nm	22.0	5.28
P3OT sps 60nm	22.0	4.80

	1435 cm^{-1} Peak	
	Peak width	Peak Amplitude
P3DT ssp 100nm	22.0	12.32
P3DT ssp 60nm	22.0	9.24
P3DT sps 100nm	22.0	4.40
P3DT sps 60nm	22.0	3.72

	1435 cm^{-1} Peak	
	Peak width	Peak Amplitude
P3DDT ssp 100nm	22.0	15.43
P3DDT ssp 60nm	22.0	12.10
P3DDT sps 100nm	22.0	3.52
P3DDT sps 60nm	22.0	3.08

Table S1 SFG spectral fitting results

From the fitting parameters listed above, χ_{ssp} and χ_{sps} from experimentally obtained spectra can be obtained. Because

$$\chi_{ssp} = F_{yyz}^{interface\ I}\chi_{yyz}^{interface\ I}e^{i\phi} + F_{yyz}^{interface\ II}\chi_{yyz}^{interface\ II} + \chi_{NR}e^{i\varphi}$$

Two χ_{ssp} terms for both 100 nm and 60 nm PT films should give two equations with same $\chi_{yyz}^{interface\ I}$ and $\chi_{yyz}^{interface\ II}$ but different $F_{yyz}^{interface\ I}$ and $F_{yyz}^{interface\ II}$. Therefore, both $\chi_{yyz}^{interface\ I}$ and $\chi_{yyz}^{interface\ II}$ can be deduced through the following equations, where all Fresnel coefficient values can be obtained from Figure 2 in the main text. Combining with the spectral fitting parameters and the corresponding Fresnel coefficients obtained, we can solve each corresponding χ term and eventually reconstruct the spectra generated from each interface:

$$\begin{cases} I_{ssp}^{100nm} = \left|0.81 \times \chi_{yyz}^{interface\ I} + 0.14 \times \chi_{yyz}^{interface\ II}\right|^2 \\ I_{ssp}^{60nm} = \left|0.56 \times \chi_{yyz}^{interface\ I} + 0.13 \times \chi_{yyz}^{interface\ II}\right|^2 \end{cases}$$

$$\begin{cases} I_{sps}^{100nm} = \left|0.14 \times \chi_{yzy}^{interface\ I} + 0.12 \times \chi_{yzy}^{interface\ II}\right|^2 \\ I_{sps}^{60nm} = \left|0.12 \times \chi_{yzy}^{interface\ I} + 0.11 \times \chi_{yzy}^{interface\ II}\right|^2 \end{cases}$$

7. SFG spectrum of DCM treated P3HT surface:

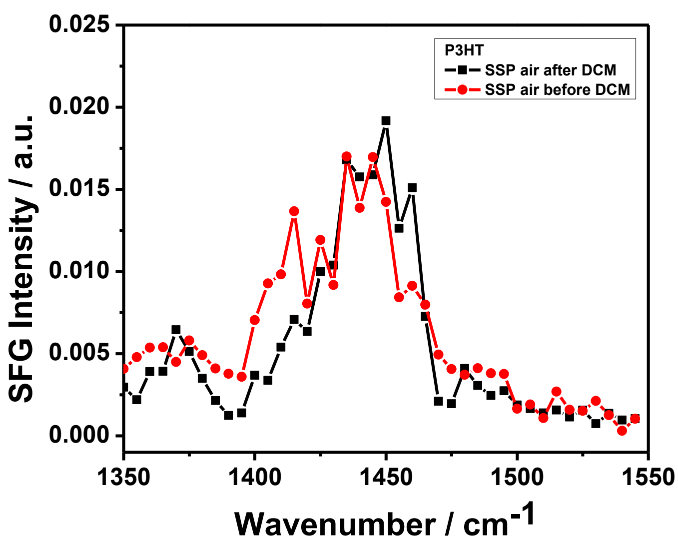

Figure S5 P3HT surface structure before and after DCM treatment

This figure shows that a P3HT surface was similar before and after the DCM solvent treatment. Such a finding is also consistent with the results about the use of DCM in the P3HT/PCBM bilayer solar cell reported previously.[1]

8. Surface morphology of perovskite solar cells fabricated:

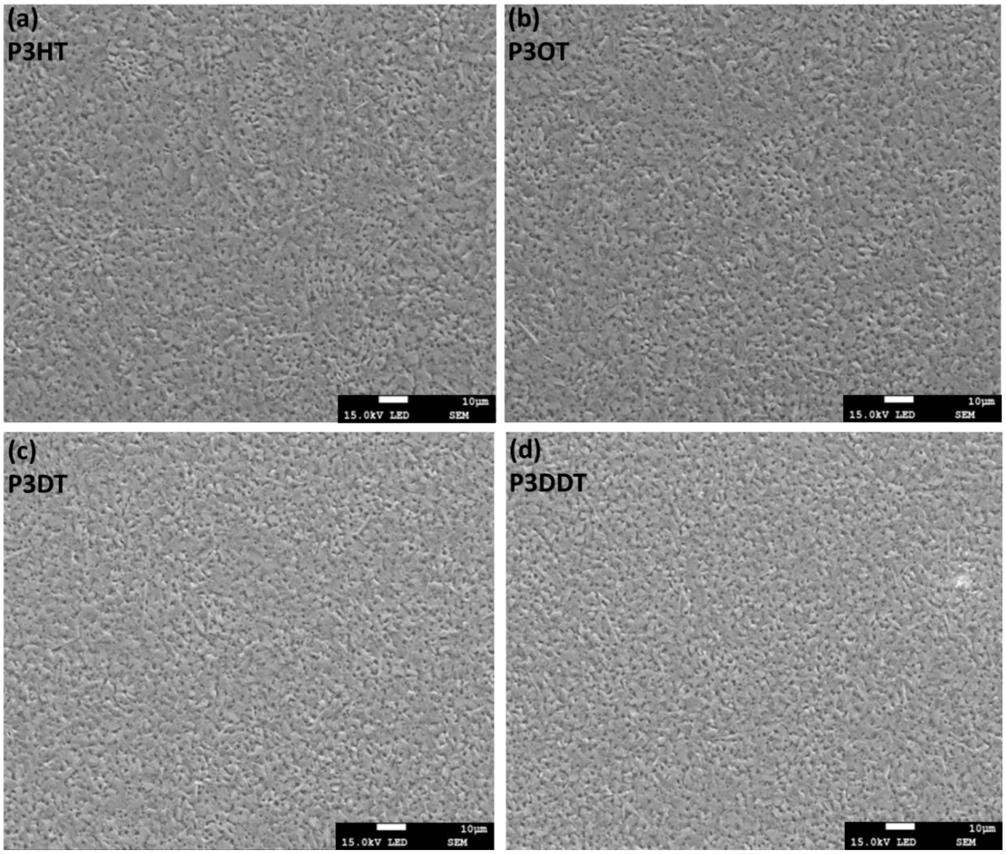

Figure S6. Surface morphologies of perovskite solar cells prepared with various PTs (a) P3HT, (b) P3OT, (c) P3DT, (d) P3DDT.

As discussed in the main text, all surfaces showed good homogeneity with visible perovskite crystal domains.

9. Average PCE:

HTL material	PCE (%)
P3HT	9.12±0.72
P3OT	6.62±0.59
P3DT	6.21±0.24
P3DDT	3.57±0.61

Table S2 Average PCE of devices fabricated with different PTs

10. Transient photovotage and transient photocurrent of perovskite solar cells fabricated:

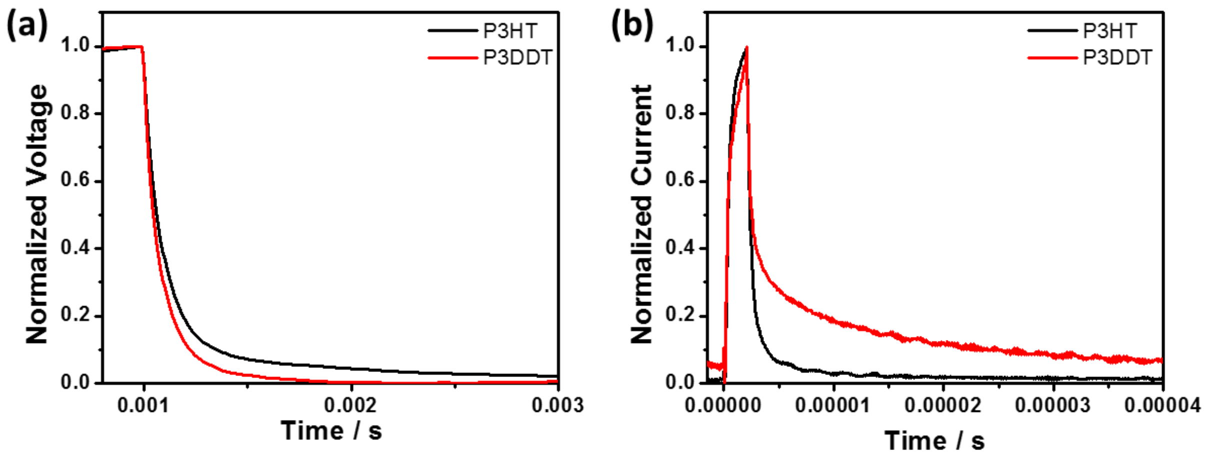

Figure S7. (a) Transient photovoltage of devices fabricated with P3HT and P3DDT under illumination; (b) Transient photocurrent of devices fabricated with P3HT and P3DDT under illumination. (All TPC and TPV measurements are conducted under the same intensity illumination)

11. PL study of perovskite/PT:

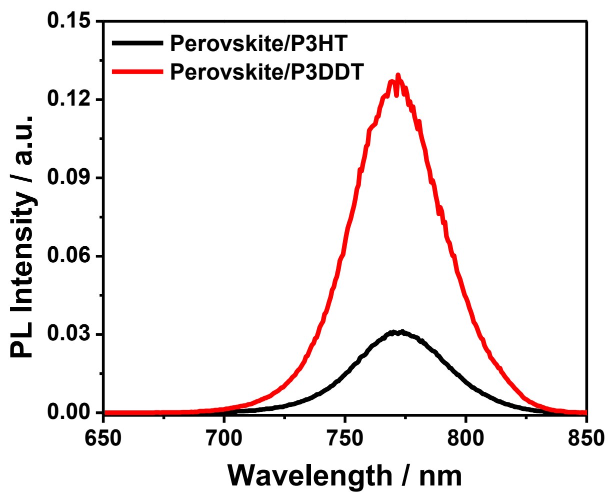

Figure S8. PL intensity of perovskite/P3HT and perovskite/P3DDT systems

12. Comparison of polythiophene crystallinity on different substrates:

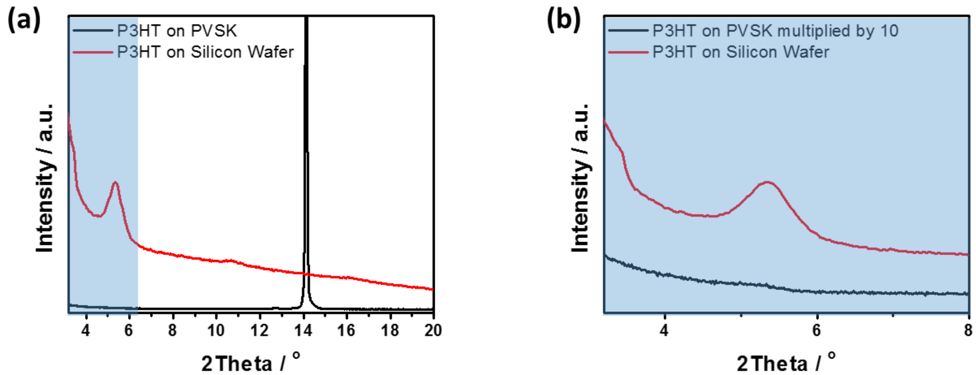

Figure S9 P3HT crystallinity on perovskite thin film and on silicon wafer

(1) Lee, K. H.; Schwenn, P. E.; Smith, A. R.; Cavaye, H.; Shaw, P. E.; James, M.; Krueger, K. B.; Gentle, I. R.; Meredith, P.; Burn, P. L. *Advanced Materials* **2011**, *23*, 766.